OPEN ACCESS Freely available online

PLoS GENETICS

Cyclin E and Cdk2 Control GLD-1, the Mitosis/Meiosis Decision, and Germline Stem Cells in *Caenorhabditis elegans*

Johan Jeong[1], Jamie M. Verheyden[2], Judith Kimble[1,2,3]*

1 Program in Cellular and Molecular Biology, University of Wisconsin–Madison, Madison, Wisconsin, United States of America, **2** Howard Hughes Medical Institute, University of Wisconsin–Madison, Madison, Wisconsin, United States of America, **3** Department of Biochemistry, University of Wisconsin–Madison, Madison, Wisconsin, United States of America

Abstract

Coordination of the cell cycle with developmental events is crucial for generation of tissues during development and their maintenance in adults. Defects in that coordination can shift the balance of cell fates with devastating clinical effects. Yet our understanding of the molecular mechanisms integrating core cell cycle regulators with developmental regulators remains in its infancy. This work focuses on the interplay between cell cycle and developmental regulators in the *Caenorhabditis elegans* germline. Key developmental regulators control germline stem cells (GSCs) to self-renew or begin differentiation: FBF RNA–binding proteins promote self-renewal, while GLD RNA regulatory proteins promote meiotic entry. We first discovered that many but not all germ cells switch from the mitotic into the meiotic cell cycle after RNAi depletion of CYE-1 (*C. elegans* cyclin E) or CDK-2 (*C. elegans* Cdk2) in wild-type adults. Therefore, CYE-1/CDK-2 influences the mitosis/meiosis balance. We next found that GLD-1 is expressed ectopically in GSCs after CYE-1 or CDK-2 depletion and that GLD-1 removal can rescue *cye-1/cdk-2* defects. Therefore, GLD-1 is crucial for the CYE-1/CDK-2 mitosis/meiosis control. Indeed, GLD-1 appears to be a direct substrate of CYE-1/CDK-2: GLD-1 is a phosphoprotein; CYE-1/CDK-2 regulates its phosphorylation *in vivo*; and human cyclin E/Cdk2 phosphorylates GLD-1 *in vitro*. Transgenic GLD-1(AAA) harbors alanine substitutions at three consensus CDK phosphorylation sites. GLD-1(AAA) is expressed ectopically in GSCs, and GLD-1(AAA) transgenic germlines have a smaller than normal mitotic zone. Together these findings forge a regulatory link between CYE-1/CDK-2 and GLD-1. Finally, we find that CYE-1/CDK-2 works with FBF-1 to maintain GSCs and prevent their meiotic entry, at least in part, by lowering GLD-1 abundance. Therefore, CYE-1/CDK-2 emerges as a critical regulator of stem cell maintenance. We suggest that cyclin E and Cdk-2 may be used broadly to control developmental regulators.

Citation: Jeong J, Verheyden JM, Kimble J (2011) Cyclin E and Cdk2 Control GLD-1, the Mitosis/Meiosis Decision, and Germline Stem Cells in *Caenorhabditis elegans*. PLoS Genet 7(3): e1001348. doi:10.1371/journal.pgen.1001348

Editor: Sue Biggins, Fred Hutchinson Cancer Research Center, United States of America

Received February 18, 2010; **Accepted** February 18, 2011; **Published** March 24, 2011

Funding: JJ was supported by the National Research Foundation (NRF) of Korea (grant #2005-215-C00111). NIH GM069454 supported this work. JK is an investigator of the Howard Hughes Medical Institute. The funders had no role in study design, data collection and analysis, decision to publish, or preparation of the manuscript.

Competing Interests: The authors have declared that no competing interests exist.

* E-mail: jekimble@wisc.edu

Introduction

Metazoan development coordinates progression through the cell cycle with key developmental events, such as stem cell maintenance, cell fate specification and patterning. An emerging theme is that core cell cycle regulators can influence development in addition to their more traditional role. For example, cyclin E affects the *Drosophila* endocycle [1,2], CDK1 influences *Drosophila* neuroblast asymmetric divisions [3] and cyclin D controls the *Caenorhabditis elegans* asymmetric division of somatic gonadal precursors [4]. Yet our understanding of the molecular interplay between cell cycle and developmental regulators remains in its infancy with only a few exceptions (e.g. MyoD and CKI [5–7]).

The *C. elegans* adult germline provides a superb model to investigate cell cycle controls in a developmental context [8]. Germ cells progress from mitotic divisions at the distal end of the adult gonad through meiotic prophase I in the middle to overt differentiation as sperm or oocyte at the proximal end. Here we focus on the distal germline, including the "mitotic zone" and adjacent "transition zone" (Figure 1A). The mitotic zone houses a pool of >200 mitotically dividing germ cells, whereas the transition zone contains germ cells that have entered the meiotic cell cycle. The transition zone is recognized by the presence of crescent-shaped DAPI-staining of nuclei, typical of the first step in pairing homologous chromosomes [9]. As germ cells move proximally through the mitotic zone, most enter meiotic S-phase prior to their entry into the transition zone [10–12]. The distal germline therefore presents an orderly maturation from stem cell through transit-amplifying cell to meiotic entry and differentiation.

Major developmental regulators controlling the choice between germline self-renewal and differentiation are well established (Figure 1B) [8]. A single somatic cell, the distal tip cell (DTC), provides the stem cell niche, and Notch signaling from the DTC drives self-renewal at the expense of meiotic entry and differentiation. Germ cells within the niche express FBF-1 and FBF-2, two nearly identical and largely redundant PUF (*Pu*milio and *F*BF) RNA-binding proteins [13,14]; the FBF proteins promote germline self-renewal and repress differentiation [15–17]. When the

Author Summary

How are cell cycle regulators coordinated with cell fate and patterning regulators during development? Several studies suggest that core cell cycle regulators can influence development, but molecular mechanisms remain unknown for the most part. We have tackled this question in the nematode *Caenorhabditis elegans*. Specifically, we have investigated how cell cycle regulators affect germline stem cells. Previous work had identified conserved developmental regulators that control the choice between self-renewal and differentiation in this tissue. In this work, we focus on cyclin E/Cdk-2, which is a core cell cycle kinase, and GLD-1, a key regulator of stem cell differentiation. Our work shows that cyclin E/Cdk-2 phosphorylates GLD-1 and lowers its abundance in stem cells via a post-translational mechanism. We also find that a post-transcriptional GLD-1 regulator, called FBF-1, works synergistically with cyclin E/Cdk-2 to ensure that GLD-1 is off in germline stem cells. When both FBF-1 and cyclin E/Cdk-2 are removed, the stem cells are no longer maintained and instead differentiate. Our findings reveal that cyclin E/Cdk-2 kinase is a critical stem cell regulator and provide a paradigm for how cell cycle regulators interface with developmental regulators.

DTC is removed by laser ablation or when GLP-1/Notch signaling or both FBFs are removed by either mutation or RNAi, germ cells leave the mitotic cell cycle, enter the meiotic cell cycle, and progress through meiotic prophase and gametogenesis [13,15,18].

Three GLD proteins and NOS-3 initiate entry into the meiotic cell cycle [10,19,20]. GLD-1 is a translational repressor [21–23], whereas the GLD-2/GLD-3 heterodimer is a translational activator [24,25] (Figure 1B). NOS-3 stimulates GLD-1 accumulation [26]. Both GLD-1 and GLD-2/GLD-3 activities must be removed to prevent entry into the meiotic cell cycle [19,20,26].

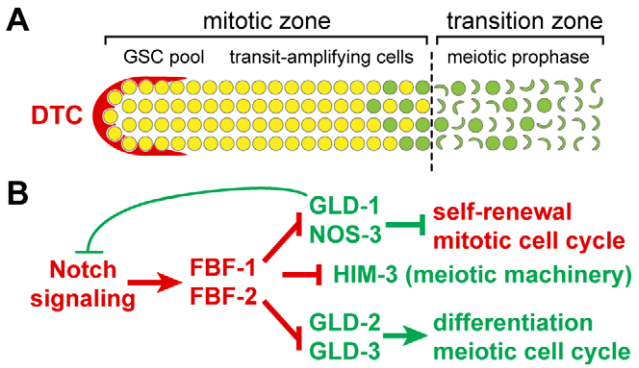

Figure 1. The mitosis/meiosis decision and its regulation. (A) Schematic of adult distal germline. The distal tip cell (DTC) niche (red) resides at the distal end. The mitotic zone contains mostly germ cells in the mitotic cell cycle (yellow) but also includes some germ cells in meiotic S-phase (green) at its proximal edge; the germline stem cell (GSC) pool is located at the distal end and consists of 30–70 germ cells. The transition zone contains germ cells in meiotic S-phase (green circles) and meiotic prophase (green crescents). The dashed line marks the boundary between mitotic and transition zones. (B) Skeleton of regulatory network controlling the decision between germline self-renewal and differentiation, a decision that also controls the choice between mitotic and meiotic cell cycles. See Introduction for details.
doi:10.1371/journal.pgen.1001348.g001

FBF is a broad-spectrum regulator of >1000 mRNAs, which include the three *gld* mRNAs [15,17,20,27]. FBF also controls many core components of the meiotic cellular machinery, including HIM-3 [17,28,29].

Most relevant here is the FBF repression of *gld-1* mRNA, which is exerted directly through a *cis*-acting regulatory element in the *gld-1* 3′ untranslated region and which is responsible for lowering *gld-1* expression in the distal mitotic zone [15,27]. In addition, the roles of FBF-1 and FBF-2 are subtly different even though they are redundant for maintenance of germline self-renewal [15,30]. For example, in *fbf-1* single mutants (but not in *fbf-2* mutants), GLD-1 is expressed ectopically in the distal-most germ cells within the niche, even though those distal germ cells remain in the mitotic cell cycle and germline self-renewal is maintained in both single mutants. Therefore, simply the presence of GLD-1 protein does not drive germ cells from the mitotic into the meiotic cell cycle [15,30].

Cyclin-dependent-kinases (CDKs) govern the cell cycle in virtually all eukaryotes, and cyclins are universal regulators of CDK activity and substrate specificity [31–34]. Phosphorylation by an active cyclin/CDK complex often affects the stability or activity of its substrates [31–35]. The *C. elegans* CDKs control cell cycle progression in both somatic and germline tissues [36–38]. Here we focus on cyclin E, which is best known as a regulator of the G1/S transition [39,40]. In *C. elegans*, the cyclin E homolog, known as CYE-1, acts with CDK-2, the Cdk2 homolog, to facilitate the G1/S transition in somatic cells and to promote proliferation of germ cells [36,41–45]. In the adult germline, CYE-1 is easily detectable throughout the mitotic zone but becomes undetectable in the transition zone and pachytene region [43]. Its presence in germ cells throughout the mitotic zone suggests that CYE-1 may have a broader role than control of the G1/S transition, because half of the mitotic zone germ cells are in S-phase [11]. In the transition zone, the GLD-1 translational repressor acts directly on *cye-1* mRNA to reduce its activity [23]. This GLD-1 control of *cye-1* mRNA translation provided the first link between developmental and cell cycle regulators in this system.

In addition to its role in cell cycle regulation, cyclin E can affect developmental events. In *C. elegans*, non-vulval cells are transformed into vulval cells upon CYE-1 removal [42], the asymmetric division of somatic gonadal precursor cells is rendered symmetrical [4] and quiescent somatic precursor cells are spurred to differentiate [45]. In *Drosophila*, cyclin E affects neuroblasts [46,47] and ovarian follicle stem cells [48]. Most recently, cyclin E has been implicated in the control of human embryonic stem cells [49]. Therefore, the coordination of cell cycle with development appears to be achieved, at least in part, by a dual role of key cell cycle regulators [39,50].

Here we report that CYE-1/CDK-2 controls the balance between proliferation and differentiation in the *C. elegans* germline, at least in part, by lowering GLD-1 abundance in dividing cells. We provide multiple lines of evidence to suggest that GLD-1 is a direct substrate of CYE-1/CDK-2 phosphorylation. These results forge a molecular and functional link between the CYE-1/CDK-2 cell cycle regulator and the GLD-1 developmental regulator. Because GLD-1 represses *cye-1* mRNA translation [23], these two regulators engage in a double negative feedback loop. Finally, we demonstrate that CYE-1/CDK-2 and FBF-1 normally function together to repress GLD-1 and prevent meiotic entry of germ cells in the stem cell pool. Therefore, CYE-1/CDK-2 emerges as a critical regulator of germline stem cell maintenance.

Results

CYE-1/CDK-2 controls the mitosis/meiosis balance in adult germlines

To assess CYE-1 function in the adult hermaphrodite germline, we placed mid to late L4 larvae on bacteria expressing double-stranded RNA (dsRNA) complementary to *cye-1* mRNA and scored germlines after 48 hours, well into adulthood. This regimen effectively reduced *cye-1* expression (Figure 2A), and is referred to henceforth as adult RNAi (aRNAi).

cye-1 aRNAi had a dramatic effect on the mitotic zone, which extends from the distal end of the adult germline along the gonadal axis to the first set of crescent-shaped nuclei in early meiotic prophase. Normally, the mitotic zone harbors actively cycling germ cells, it extends 18–20 germ cell diameters (gcd) along the gonadal axis from the distal end, and its total germ cell number exceeds 200 [51]. However, after *cye-1* aRNAi, this region was abnormal: germ cell nuclei were grossly enlarged (Figure 2A–2C), the mitotic index plummeted from 3% to 0.5% (Figure 2E), the length of the region, measured in gcd from the distal end, was reduced from 19 gcd in controls to 12 gcd (Figure 2A, 2D), and total number of germ cells was reduced from 219 to 77 (Figure 2F). After 72 or 94 hrs of *cye-1* aRNAi treatment, these abnormal distal germ cells began to deteriorate (Figure S1A). Similar results were obtained after *cdk-2* aRNAi (Figure 2D–2F). Therefore, CYE-1 and CDK-2 appear to act together to keep about one-third of the germ cells in the mitotic zone from enlarging abnormally and to prevent the remaining two-thirds from entering meiotic prophase.

We wondered if the enlarged distal germline nuclei might reflect partial rather than full depletion of CYE-1/CDK-2 activity. A *cye-1* null mutant or *cye-1* RNAi treatment at an early stage in larval development affects both somatic and germ cell divisions [42]; moreover, somatic cells control germ cell proliferation [52,53]. We therefore turned to other methods to address this issue. First, we enhanced aRNAi with *eri-1* and *rrf-3* mutants [54,55]; however, the mitotic zone length was still shorter after *cye-1* depletion (Figure S1B) and enlarged distal germ cells were still observed. Second, we restricted RNAi to the germline using *rrf-1* mutants, which are defective for somatic but not germline RNAi; this mutant therefore permitted CYE-1 depletion in young larvae without affecting somatic divisions [55]. However, *cye-1* RNAi treatment initiated in *rrf-1* first stage larvae (L1s) again resulted in typical distal germline defects (Figure S1B). Third, we generated a genomic *cye-1* transgene, *qIs134* (Figure S2A), using a method predicted to allow expression in somatic cells but not germ cells [56] (see Experimental Procedures). Consistent with that prediction, CYE-1 protein was detected in somatic but not germ cells of *cye-1(0); qIs134* embryos (Figure S2B) and *qIs134* rescued *cye-1(0)* somatic defects (Figure S2C). However, germlines in these somatically rescued *cye-1(0); qIs134* animals were smaller than normal, with abnormally enlarged distal germ cells (Figure S2D, bottom), as seen previously in *cye-1* null mutants [41–43]. Therefore, the enlarged germline nuclei observed after *cye-1* and *cdk-2* aRNAi are likely to represent the effect of eliminating CYE-1/CDK-2 activity. In addition, these experiments show that CYE-1 functions autonomously within germ cells.

We next attempted to ask if the enlarged distal germ cells were in the mitotic or meiotic cell cycle. To this end, we first stained for cytoplasmic REC-8, a marker of mitotic germ cells [10], and chromosomal HIM-3, a marker of meiotic germ cells [28]. In most *cye-1(aRNAi)* germlines (97.1%, n = 35), REC-8 was lower in the mitotic zone relative to controls (Figure 2B) and HIM-3 expanded distally (82.5%, n = 40; Figure 2C). This shift in marker distribution suggested that the enlarged distal germ cells may have entered the meiotic cell cycle. However, the finite mitotic index, albeit low, suggested that at least some germ cells remained in the mitotic cell cycle. To explore this question further, we examined DNA content of DAPI-stained nuclei, comparing values for the abnormally enlarged germline nuclei to those of nuclei in the somatic DTC (2n) and pachytene germ cells (4n). This analysis revealed a range of DNA content from 2n to 4n in the abnormally enlarged germline nuclei that was essentially the same as seen in wild-type mitotic zone nuclei (Figure 2G). DNA content therefore does not distinguish between germ cells being in mitotic or meiotic S-phase.

Figure 2H depicts one interpretation of the phenotype typical of *cye-1(aRNAi)* distal germlines. The wild-type mitotic zone contains >200 germ cells in the mitotic cell cycle (Figure 2H, above). However, the *cye-1(aRNAi)* "mitotic zone" contains only ~75 enlarged germ cells whose state is questionable (Figure 2H, below). Figure 2H suggests that the distal most ~75 germ cells enlarge after *cye-1* depletion while the more proximal >100 germ cells enter meiotic prophase prematurely (Figure 2H, dashed lines between wild-type and *cye-1(aRNAi)* distal germlines). An alternative explanation might have been that >100 germ cells die, but no germ cell corpses or degenerating germ cells were seen during the transition from the wild-type >200 germ cells mitotic zone to the *cye-1(aRNAi)* ~75 germ cells mitotic zone. A third possibility is that the 75 enlarged germ cells come from some other part or parts of the mitotic zone and that the remaining germ cells are squeezed proximally as the ~75 enlarge. Regardless, we conclude that *cye-1* depletion causes ~75 of the >200 germ cells in the mitotic zone to enlarge abnormally and that it also causes the remaining >100 germ cells in the mitotic zone to enter meiotic prophase. Therefore, CYE-1/CDK-2 is required to achieve and maintain the normal balance between numbers of germ cells in the mitotic and meiotic cell cycles.

CYE-1/CDK-2 acts through GLD-1 to control distal germ cells

We postulated that CYE-1/CDK-2 might exert its influence in the mitotic zone through GLD-1, a key repressor of germline proliferation (see Introduction). We first tested for a change in GLD-1 abundance after CYE-1/CDK-2 depletion. In wild-type and control germlines, GLD-1 was barely detectable in the distal mitotic zone, increased in the proximal mitotic zone and became abundant in the transition zone (Figure 3A, top), as seen previously [26,57]. By contrast, GLD-1 was abundant throughout the mitotic zone in both *cye-1(aRNAi)* and *cdk-2(aRNAi)* germlines (Figure 3A, middle and bottom). A similar GLD-1 increase was also observed in *gld-1(q361)* homozygotes (Figure S3A, S3B), which harbor a G227D point mutation in the KH domain resulting in loss of GLD-1 function [58]. Therefore, the GLD-1 increase upon CYE-1/CDK-2 depletion is not dependent on GLD-1 function. We conclude that CYE-1 and CDK-2 lower the abundance of GLD-1 in the wild-type mitotic zone.

To ask genetically if CYE-1/CDK-2 might function through GLD-1 in the mitotic zone, we depleted CYE-1 or CDK-2 in *gld-1* null mutant germlines. Remarkably, the *cye-1/cdk-2* defects disappeared in both *gld-1; cye-1(aRNAi)* and *gld-1; cdk-2(aRNAi)* distal germlines: cells were not abnormally enlarged and HIM-3 failed to extend distally (Figure 3B, upper panels). Instead germ cells in the mitotic zone appeared similar to those in the *gld-1* control. Furthermore, mitotic zone lengths were equivalent in *gld-1(0)*, *gld-1; cye-1(aRNAi)* and *gld-1; cdk-2(aRNAi)* (Figure 3B, 3D). The possibility that *gld-1* mutants might be ineffective for RNAi was ruled out in two ways. First, the amount of CYE-1 protein was sharply reduced in the mitotic zone of *gld-1; cye-1(aRNAi)* germlines

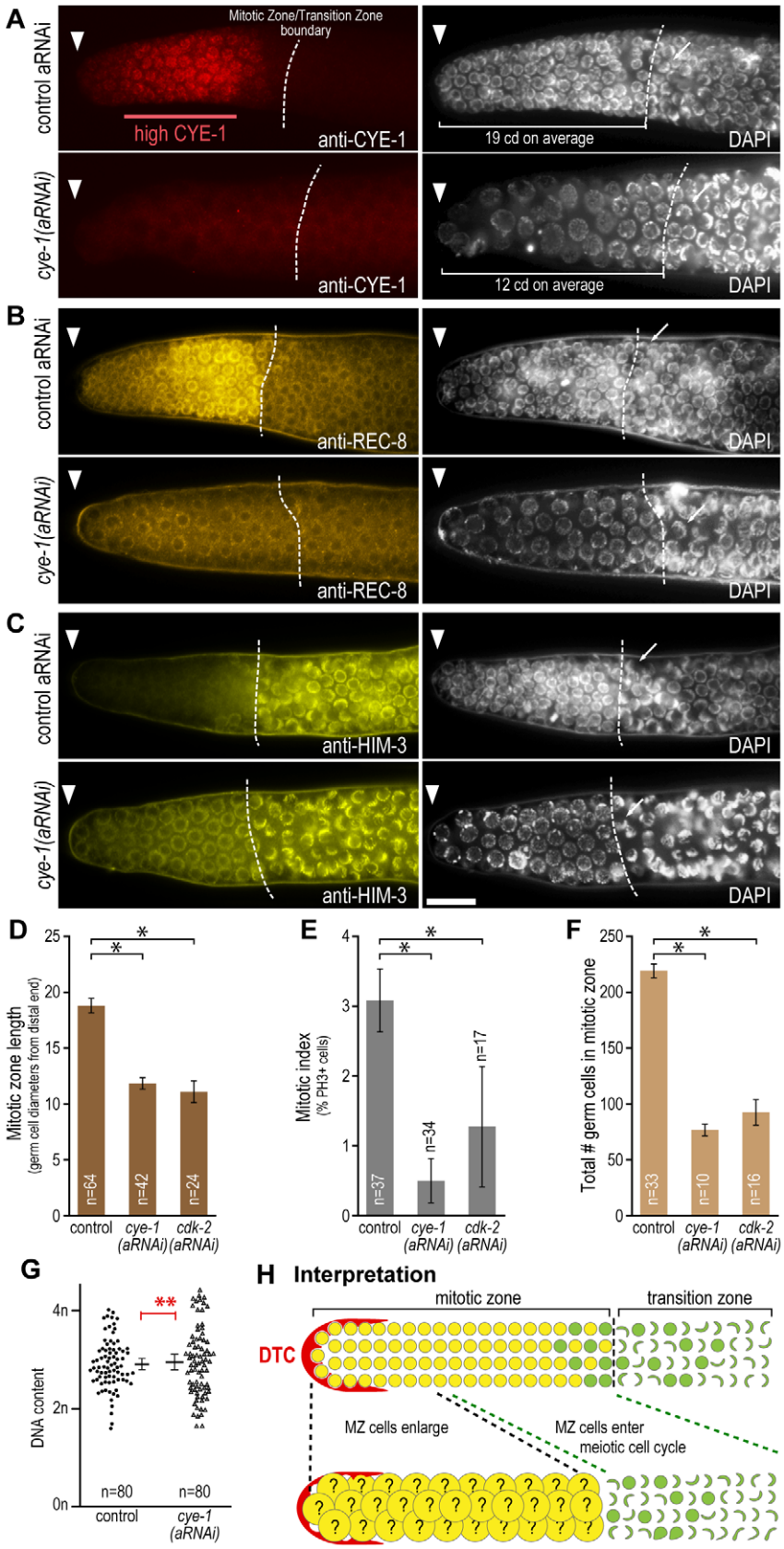

Figure 2. CYE-1/CDK-2 controls the mitosis/meiosis balance. (A–C) Dissected gonads stained with antibodies (left panels) and DAPI (right) after aRNAi treatment for 48 hrs from L4. Arrowhead, distal end of the gonad; dashed line, boundary between mitotic and transition zones; arrows, nuclei with crescent-shape typical of meiotic prophase. Right/left images are the same gonad; germlines in each panel were treated identically and

fluorescent images taken at the same settings. Scale bar, 20 μm. (A) CYE-1 staining decreases dramatically after *cye-1* aRNAi. (B) REC-8 decreases after *cye-1* aRNAi. (C) HIM-3 increases after *cye-1* aRNAi. (D–G) *cye-1* and *cdk-2* aRNAi effects on features of mitotic zone; error bars indicate 95% confidence limits; one asterisk denotes a statistically significant difference ($p<0.0006$ using Student's *t*-test); two asterisks denote the lack of a statistically significant difference ($p>0.6$ using Student's *t*-test). (D) Mitotic zone length; (E) mitotic index; (F) germ cell number; (G) germ cell DNA content. (H) Interpretation. Above, diagram of wild-type distal germline; below, diagram of *cye-1(aRNAi)* or *cdk-2(aRNAi)* germline. Enlarged germ cells (yellow with question mark) have features of both mitotic and meiotic cells. Dashed lines, one interpretation for how wild-type mitotic zone may reduce its germ cell number. See text for explanation and other interpretations.
doi:10.1371/journal.pgen.1001348.g002

(Figure S4); second, germ cells in the proximal loop region appeared cell cycle arrested instead of tumorous in *gld-1; cye-1(aRNAi)* germlines (Figure 3B, bottom panels). We conclude that GLD-1 is required for *cye-1(aRNAi)* and *cdk-2(aRNAi)* defects in the mitotic zone.

GLD-1 is one of several genes affecting meiotic entry and meiotic progression (Figure 1B) [8]. We therefore asked if others might be similarly epistatic to *cye-1* defects in the mitotic zone, but this was not the case. For example, *him-3; cye-1(aRNAi)* mitotic zones were similar to those of *cye-1(aRNAi)*: GLD-1 expanded distally (Figure 3C, left), germ cells enlarged (Figure 3C, right), and the zone was shortened relative to controls (Figure 3D, right). Similarly, *cye-1(aRNAi)* depletion in *gld-2*, *gld-3*, and *nos-3* null mutants resulted in typical *cye-1* mitotic zone defects. We conclude that CYE-1/CDK-2 acts through GLD-1 to regulate germ cell number and size in the mitotic zone.

CYE-1/CDK-2 likely phosphorylates GLD-1

We next considered the idea that GLD-1 protein might be a direct target of the CYE-1/CDK-2 kinase. This prospect seemed plausible because the GLD-1 amino acid sequence possesses three consensus CDK phosphorylation sites (X-X-X-S/T-P-X-K/R) [59,60] (Figure 4A and 4B, red) and four predicted cyclin binding sites (R/K-X-L-(X)-F/Y/L/I/V/M/P) [61,62] (Figure 4A and 4B, blue). To ask if GLD-1 is a phosphoprotein, we examined GLD-1 on Western blots, with or without phosphatase treatment (Figure 4C). The GLD-1 antibody recognized two bands in proteins prepared from wild-type extracts (Figure 4C, left panel). Although the resolution of these two bands was not optimal and the lower band was much more abundant, phosphatase treatment reduced the upper band whereas phosphatase inhibitor restored it (Figure 4C, left panel).

We reasoned that the relative amount of phosphorylated GLD-1 might be low in wild-type extracts, because CYE-1 and GLD-1 only overlap in a small region within the proximal part of the mitotic zone (Figure S5A), whereas abundant GLD-1 extends over a much larger region [23,43,57]. In an attempt to increase the ratio of phosphorylated to unphosphorylated GLD-1, we used *gld-3(0) nos-3(0)* double mutants, which have a germline tumor [20] with broadly distributed CYE-1 and less GLD-1 overall (Figure S5B). Before assaying phosphorylation, we confirmed that CYE-1/CDK-2 influences GLD-1 abundance in the *gld-3 nos-3* tumorous germline (Figure 4E). We then prepared extracts from the double mutants and assayed GLD-1 phosphorylation. The two GLD-1 bands were better resolved in the *gld-3 nos-3* extracts (Figure 4C, right), and again phosphatase treatment reduced the upper band while phosphatase inhibitor restored it (Figure 4C, right panel). Finally, we assayed proteins from *gld-3 nos-3* mutants after treatment with *cye-1* or *cdk-2* aRNAi and found that phosphorylated GLD-1 was indeed reduced (Figure 4D). We conclude that GLD-1 is a phosphoprotein and that its phosphorylation depends on CYE-1 and CDK-2 *in vivo*.

To ask if GLD-1 might be a direct substrate of CYE-1/CDK-2 phosphorylation, we used a commercially available cyclin E/CDK2 complex. We incubated full-length GLD-1 recombinant protein prepared from *E. coli* with purified human cyclin E/CDK2 complex (Cell Signaling) and radiolabelled ATP. As expected, cyclin E/CDK2 phosphorylated the positive control histone H1 but not the negative control BSA (Figure 4F, lanes 1–4). More importantly, the complex phosphorylated wild-type GLD-1(wt) (Figure 4F, lane 5), but not a mutant, GLD-1(AAA), which had its three putative CDK phosphorylation site residues substituted to alanines (S22A, S39A, T348A) (Figure 4F, lane 7). We conclude that human cyclin E/CDK2 directly phosphorylates GLD-1 *in vitro*.

GLD-1 CDK phosphorylation sites affect its abundance and mitotic zone size

To ask if CYE-1/CDK-2 controls GLD-1 abundance via its predicted phosphorylation sites, we generated transgenes encoding a GFP- and FLAG-tagged GLD-1 that was either wild-type or mutated at its putative CDK phosphorylation sites [dubbed transgenic (tr) GLD-1(wt) and trGLD-1(AAA), respectively] (Figure 5A). Both trGLD-1(wt) and trGLD-1(AAA) made functional protein, as assayed by *gld-1(0)* mutant rescue to fertility. The distribution of the transgenic proteins was analyzed in five independent lines for each protein with equivalent results. Expression of the trGLD-1(wt) protein was very low or undetectable in the distal mitotic zone (Figure 5B, top), but trGLD-1(AAA) was easily seen (Figure 5B, bottom). Indeed, the abundance of trGLD-1(AAA) in the distal germline was greater than that of trGLD-1(wt), when quantified using ImageJ (Figure 5C). The mitotic zone length in trGLD-1(AAA) germlines was also shorter: 13.9 gcd on average in trGLD-1(AAA) germlines (n = 40) compared to 17.8 gcd on average in trGLD-1(wt) control germlines (n = 36) (Figure 5B, 5D). A similar effect was observed in a *gld-1(0* mutant background, both with respect to higher protein abundance at the distal end and shortening of the mitotic zone (Figure S8). We note however that *cye-1* depletion increased trGLD-1(AAA) in the distal-most germ cells even more (Figure S9), suggesting that CYE-1/CDK-2 represses GLD-1 abundance both directly and indirectly. We also measured total transgenic GLD-1 protein with anti-GLD-1 antibodies in Western blots, and total transgenic *gld-1* mRNA with primers to the *gfp* portion of the mRNA. The total trGLD-1(AAA) protein was twice as abundant as total trGLD-1(wt) protein (Figure 5E), but mRNA levels were comparable (Figure 5F). We conclude that the CDK phosphorylation sites in GLD-1 contribute to the control of its abundance in the distal germline and also contribute to control of mitotic zone length.

CYE-1/CDK-2 works with FBF-1 to maintain germline stem cells

Earlier work showed that FBF-1 and FBF-2 repress *gld-1* expression in the distal germline [15], and this work shows that CYE-1/CDK-2 lowers GLD-1 abundance in the same region. To ask if these two controls might function synergistically to control cell fate in the distal germline, we treated wild-type, *fbf-1(0)* and *fbf-2(0)* single mutants with *cye-1* aRNAi and examined their mitotic zones as described earlier. The distal-most germ cells did

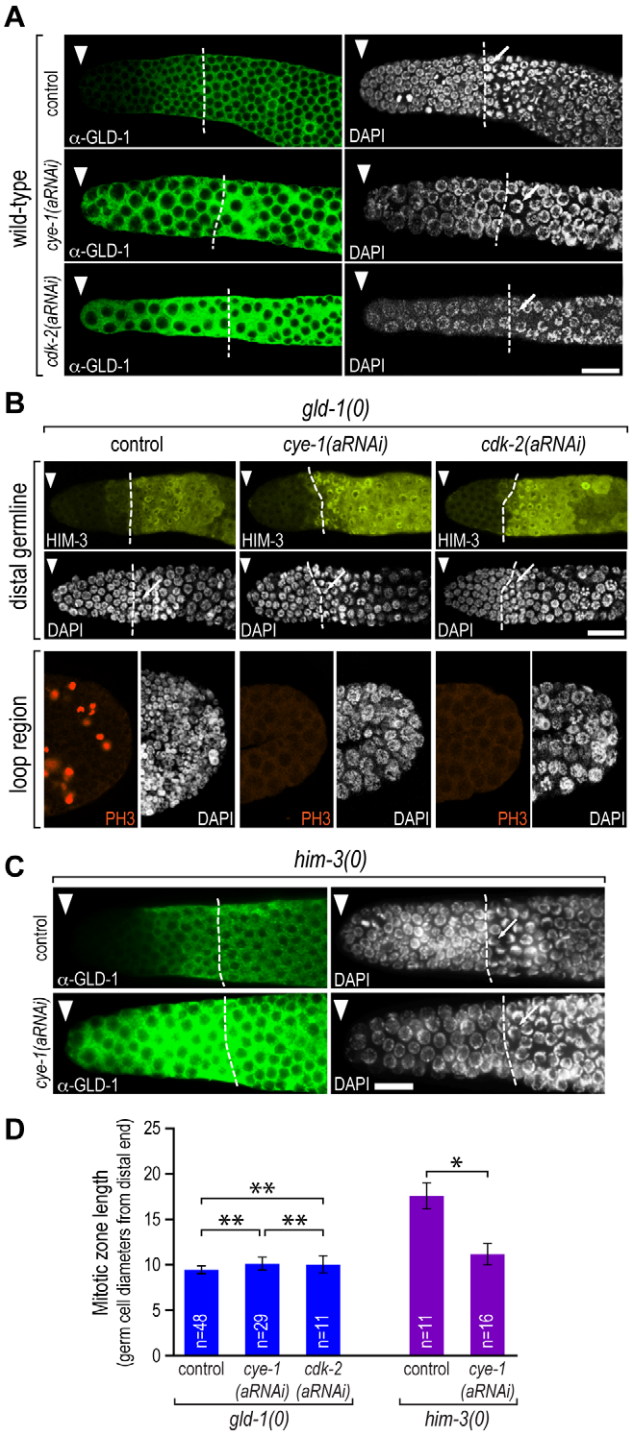

Figure 3. CYE-1/CDK-2 effects on distal germline are GLD-1–dependent. (A–C) Dissected gonads stained after aRNAi treatment for 48 hrs from L4 (conventions same as Figure 2). Right/left images are the same gonad in A and C; columns have the same gonad in B; germlines in each panel were treated identically and fluorescent images taken at the same settings. Scale bar, 20 μm. (A) Wild-type. GLD-1 abundance increases in the distal germline after *cye-1* or *cdk-2* aRNAi. (B) *gld-1* null mutant. Distal germline (top) or loop region, where germ cells normally begin overt oogenesis (bottom). In the absence of GLD-1, HIM-3 does not increase and germ cells do not enlarge in the distal germline after *cye-1* or *cdk-2* aRNAi. In the loop region, germ cells enlarge after *cye-1* or *cdk-2* aRNAi, showing that RNAi was effective. (C) *him-3* null mutant. GLD-1 abundance increases (left) and germ cells enlarge (right) in the distal germline after *cye-1* aRNAi. (D) Mitotic zone length in wild-type, *gld-1(0),* and *him-3(0)* mutants after treatment with control, *cye-1* or *cdk-2* aRNAi for 48 hrs from L4, as noted in the figure. Error bars indicate 95% confidence limits; one asterisk denotes a statistically significant difference ($p<1.5\times E^{-7}$ using Student's *t*-test); two asterisks denote the lack of a statistically significant difference ($p>0.11$ using Student's *t*-test).

doi:10.1371/journal.pgen.1001348.g003

not enter meiotic prophase in *cye-1(aRNAi)* animals (shown above: Figure 3A, right). However, in *fbf-1(0); cye-1(aRNAi)* germlines, the distal-most germ cells acquired crescent-shaped DAPI-staining typical of meiotic prophase (Figure 6A, middle panel, right); the distal germ cells similarly entered meiotic prophase in *fbf-1(0); cdk-2(aRNAi)* germlines (Figure 6A, bottom panel, right). However, *fbf-2(0)* mutants behaved like wild-type after either *cye-1* aRNAi or *cdk-2* aRNAi (Figure 6B). We conclude that the combined action of the CYE-1/CDK-2 and FBF-1 prevents the distal germ cells from entering into meiotic prophase.

To ask whether FBF-1 and CYE-1 normally function together to lower GLD-1 in the distal germline, we quantitated GLD-1 protein in confocal images of wild-type, *fbf-1*, and *fbf-2* germlines, each treated with control, *cye-1*, or *cdk-2* aRNAi (Figure 6C–6E). Two equivalent positions were scored: the distal-most region corresponding to what normally is the germline stem cell pool and a more proximal region corresponding to what normally is the transition zone ("distal" and "proximal" squares in Figure 6C). GLD-1 was significantly more abundant in *fbf-1(0); cye-1(aRNAi)* and *fbf-1(0); cdk-2(aRNAi)* than in the equivalent position of controls (Figure 6D, middle). Indeed, the GLD-1 was more abundant in *fbf-1(0); cye-1(aRNAi)* and *fbf-1(0); cdk-2(aRNAi)* distal germ cells than in any region of control germlines (Figure 6D and 6E). Comparison of GLD-1 abundance in more proximal regions revealed only minor differences (Figure 6E). In contrast to *fbf-1(0)*, we found no dramatic increase of GLD-1 in *fbf-2(0); cye-1(aRNAi)* germlines (Figure 6B, 6D, 6E). We conclude that the combined action of CYE-1/CDK-2 and FBF-1 maintains the extremely low GLD-1 abundance typical of wild-type distal-most germ cells. This combined action may work directly on GLD-1, indirectly through other proteins or perhaps most likely through action on both GLD-1 and other proteins in the network.

GLD-1 is normally repressed in self-renewing germ cells [15]. To test if entry into meiotic prophase in the distal-most *fbf-1(0); cye-1(aRNAi)* germ cells might rely on high GLD-1, we examined the effect of varying *gld-1* dosage. We first examined germlines lacking GLD-1, and found that entry into meiotic prophase did not occur in the distal-most cells of *gld-1(0); fbf-1(0)* or *gld-1(0); fbf-1(0); cye-1(aRNAi)* germlines (Figure S6, upper and middle panels). This result is consistent with both CYE-1/CDK-2 and FBF-1 acting upstream of GLD-1 to prevent entry into meiotic prophase. Next we tested a germline with a single dose of wild-type *gld-1*: again entry into meiotic prophase did not occur in the distal-most cells in *gld-1(0)/+; fbf-1(0); cye-1(aRNAi)* germlines (Figure S6, bottom). Therefore, the entry into meiotic prophase observed in the *fbf-1(0); cye-1(aRNAi)* distal-most germ cells (Figure 6A) is suppressed by lowering GLD-1 to either a null or heterozygous state. We conclude that two copies of wild-type *gld-1* are required to drive the distal-most germ cells into meiotic prophase when CYE-1 is depleted in *fbf-1* mutants.

Distinct effects of CDK-1 and CDK-2 on the mitosis/meiosis decision

CDK-1 is the *C. elegans* homolog of mammalian CDK1 and is required for M-phase, in both somatic and germline tissues [44].

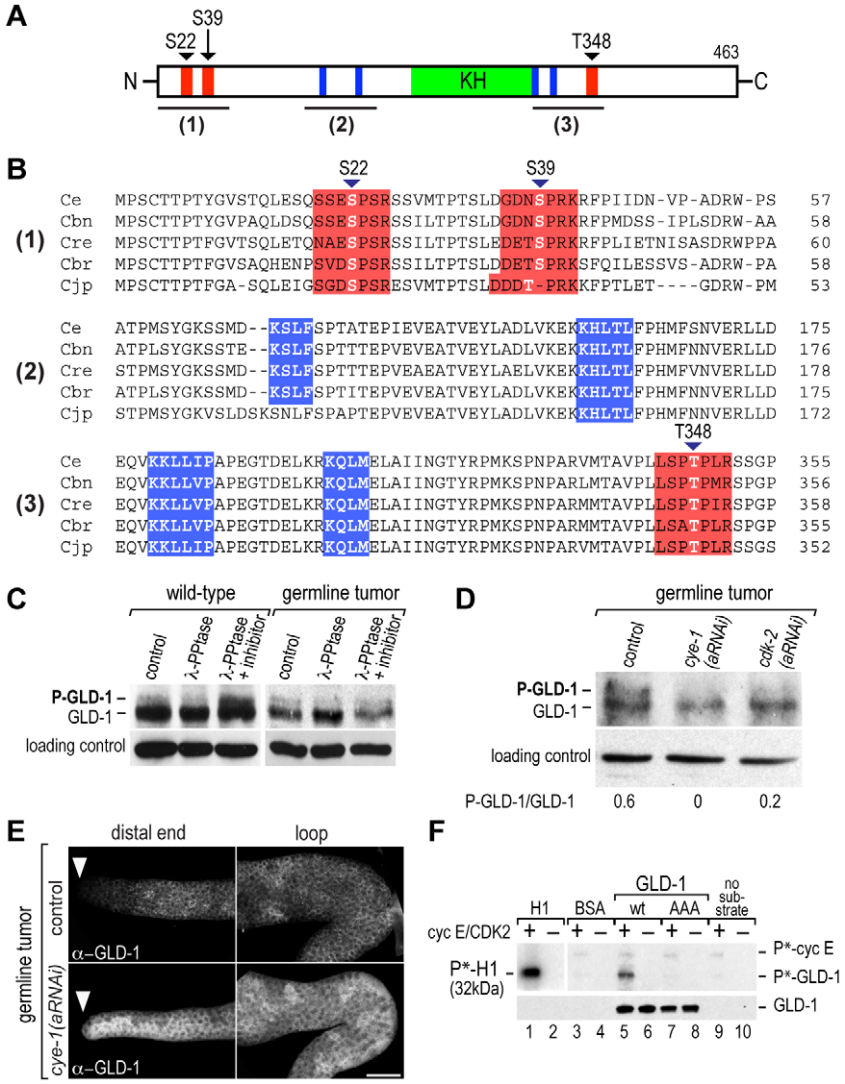

Figure 4. GLD-1 is a likely substrate of the CYE-1/CDK-2 complex. (A) Schematic of motifs in GLD-1 protein: three predicted CDK phosphorylation sites (red), four predicted cyclin binding sites (blue), and the KH domain (green). (B) Alignment of three regions of GLD-1 amino acid sequence (locations of 1, 2 and 3 shown in A) from five nematode species using MAFFT (v.6.624b, http://align.bmr.kyushuu.ac.jp/mafft/online/server/). Ce, *C. elegans*; Cbn, *C. brenneri*; Cre, *C. remanei*; Cbr, *C. briggsae*; Cjp, *C. japonica*. Red boxes, predicted CDK phosphorylation sites with predicted phosphorylation residues in white bold. Blue boxes, putative cyclin binding sites. (C) GLD-1 is a phosphoprotein. Western blots of extracts prepared from wild-type adults (left) or *gld-3 nos-3* mutant adults with a germline tumor (right). Lanes include untreated control and treatment with Lambda Protein Phosphatase (λ PPtase, NEB) either with or without Halt Phosphatase Inhibitor Cocktail (Thermo Scientific). Top panel, GLD-1; bottom panel, actin loading control. (D) CYE-1/CDK-2 is required *in vivo* for GLD-1 phosphorylation. Western blots of extracts prepared from *gld-3 nos-3* tumorous mutants treated with control, *cye-1* or *cdk-2* aRNAi. Top, GLD-1; middle, actin; bottom, relative band intensities quantified using ImageJ. (E) CYE-1/CDK-2 reduces the abundance of GLD-1 in the germline. Confocal images of dissected germlines stacked through Z-axis. Top, *gld-3 nos-3* control; bottom, *gld-3 nos-3; cye-1(aRNAi)*. Germlines were treated identically and fluorescent images taken at the same settings. Scale bar, 20 μm. (F) Human cyclin E/CDK2 phosphorylates wild-type (wt) GLD-1 *in vitro*, but does not phosphorylate a GLD-1(AAA) mutant with its predicted sites of CDK phosphorylation substituted with alanine (S22A, S39A and T348A). Above, P32 incorporation. P*-GLD-1 marks GLD-1; P*-cyclin E marks auto-phosphorylation; P*-H1 marks Histone H1 positive control; BSA was the negative control. Below, Western blot showing GLD-1 input.
doi:10.1371/journal.pgen.1001348.g004

Like *cdk-2* aRNAi, CDK-1 depletion shortened the mitotic zone (Figure S7A and S7B), as shown previously [44]. However, this *cdk-1* effect was not accompanied by an expansion of GLD-1 to the distal end (95%, n = 21) (Figure S7A, top), and it was not synergistic with *fbf-1(0)* or *fbf-2(0)* mutants (Figure S7A and S7B). Most importantly, the distal-most germ cells in *fbf-1(0); cdk-1(aRNAi)* did not acquire crescent-shaped nuclei typical of meiotic prophase, even though they were enlarged (Figure S7A, middle, and S7B). Similarly aRNAi depletion of CDK-4, CYA-2 and CYB-1 did not mimic *cye-1/cdk-2* effects. We suggest that CDK-1 functions in the germline as a core cell cycle regulator of M-phase, but does not repress the developmental regulator GLD-1.

Discussion

This work explores the role of CYE-1 and CDK-2 in the *C. elegans* germline and comes to two major conclusions. First, CYE-1 and CDK-2 regulate the mitosis/meiosis balance, and do so, at least in part, by downregulating abundance of the GLD-1 translational repressor. Second, CYE-1 and CDK-2 work together

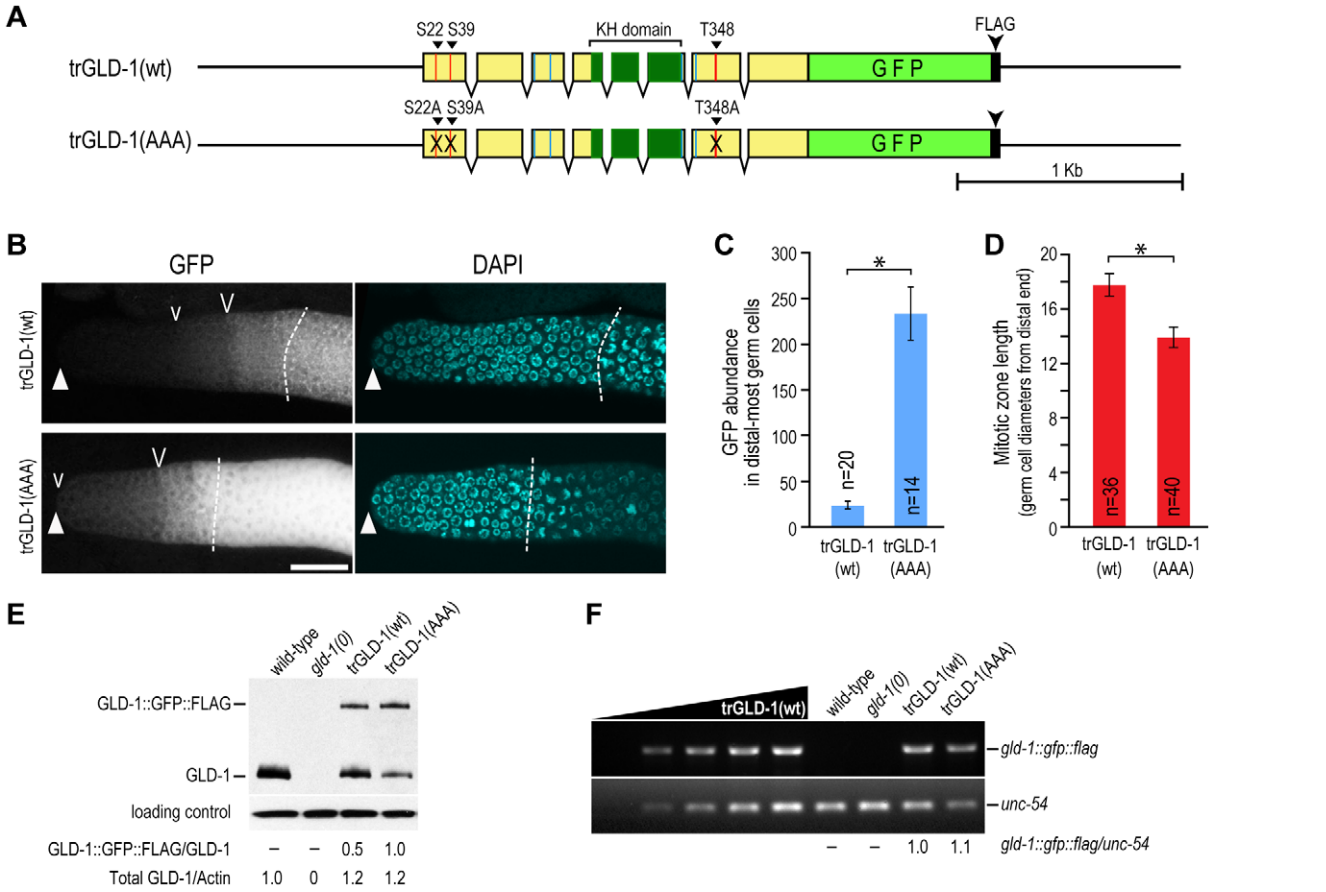

Figure 5. CDK phosphorylation sites contribute to GLD-1 regulation *in vivo*. (A) Schematics of *gld-1* transgenes. Above, transgenic (tr) GLD-1 with wild-type (wt) sequence; below, GLD-1(AAA) had its predicted sites of CDK phosphorylation substituted with alanine (S22A, S39A and T348A). Cyclin binding sites, blue lines. (B–E) CDK phosphorylation influences both GLD-1 abundance in the distal germline and the mitotic zone length. (B) Distal end of dissected gonads with DAPI staining. Left panels, GFP fluorescence reports transgenic GLD-1; right panels, DAPI staining reveals boundary between mitotic and transition zones. Solid triangle marks distal end; v and V mark steps of comparable GLD-1 abundance; dashed line is boundary between mitotic and transition zones. Germlines were treated identically and confocal fluorescent images taken at the same settings and then stacked through Z-axis. Scale bar, 20 μm. (C) ImageJ quantitation of GFP in the distal-most germline. Units on y-axis refer to pixel intensity; background was subtracted from both measurements. Error bars indicate 95% confidence limits; asterisk denotes a statistically significant difference ($p<4.4\times E^{-6}$ using Student's *t*-test). (D) Mitotic zone length is reduced in trGLD-1(AAA) compared to trGLD-1(wt). Error bars indicate 95% confidence limits; asterisk denotes a statistically significant difference ($p<7.3\times E^{-10}$ using Student's *t*-test). (E) Total trGLD-1(AAA) is higher than total trGLD-1(wt). Western blots of proteins prepared at 48 hrs after L4. Top panel, GLD-1 antibodies detect both transgenic GLD-1 (upper band) and endogenous GLD-1 (lower band); middle panel, actin; bottom panel, quantitation of band intensities, measured with ImageJ and analyzed with Microsoft Excel. (F) Transgenic *gld-1(wt)* and *gld-1(AAA)* mRNAs were of comparable abundance. mRNAs were extracted at 48 hrs after L4 stage, cDNA synthesized by RT-PCR, and DNA fragments were amplified using primers against a GFP-encoding part of transgenic mRNA and against *unc-54* for a control. Quantitation of PCR products was done using KODAK MI program.
doi:10.1371/journal.pgen.1001348.g005

with FBF-1 to prevent cells in the germline stem cell pool from precocious meiotic entry and differentiation. Our discussion places these findings in context with previously known controls of the mitosis/meiosis decision and stem cell maintenance.

The GLD-1 developmental regulator is likely a direct CYE-1/CDK-2 substrate

GLD-1 normally facilitates the switch of germ cells from the mitotic cell cycle into the meiotic cell cycle (see Introduction). In wild type, the GLD-1 protein is either extremely low or absent in the germline stem cell pool, but after depletion of either CYE-1 or CDK-2, GLD-1 becomes abundant in the distal-most germ cells. That GLD-1 increase is not simply a reflection of a mitotic cell cycle defect since depletion of other cell cycle regulators (e.g. CDK-1, CDK-4, CYA-2, EMB-30) does not lead to a similar GLD-1 increase in the distal germline (this work and [63]). Therefore, CYE-1/CDK-2 appears to govern GLD-1 independently of its canonical role in the cell cycle.

Several lines of evidence suggest that GLD-1 is a direct substrate of CYE-1/CDK-2. First, endogenous GLD-1 is a phosphoprotein, as shown here and corroborated by mass spectrometry [64]. Indeed, CDK-2 was predicted to be the best candidate kinase for the GLD-1 peptides identified in the *C. elegans* phosphoproteome [64]. Second, GLD-1 phosphorylation depends on CYE-1 and CDK-2 *in vivo*, and human cyclin E/CDK2 phosphorylates GLD-1 *in vitro*. Third, transgenic GLD-1 with serine/threonine to alanine substitutions at predicted CDK phosphorylation sites is ectopically expressed in the distal germline. Yet no obvious cell cycle perturbation was observed in the transgenic GLD-1(AAA) germlines, supporting the suggestion that GLD-1 phosphorylation represents a cell cycle independent role of CYE-1/CDK-2. Intriguingly, cyclin B/Cdk1 phosphorylates a mammalian GLD-

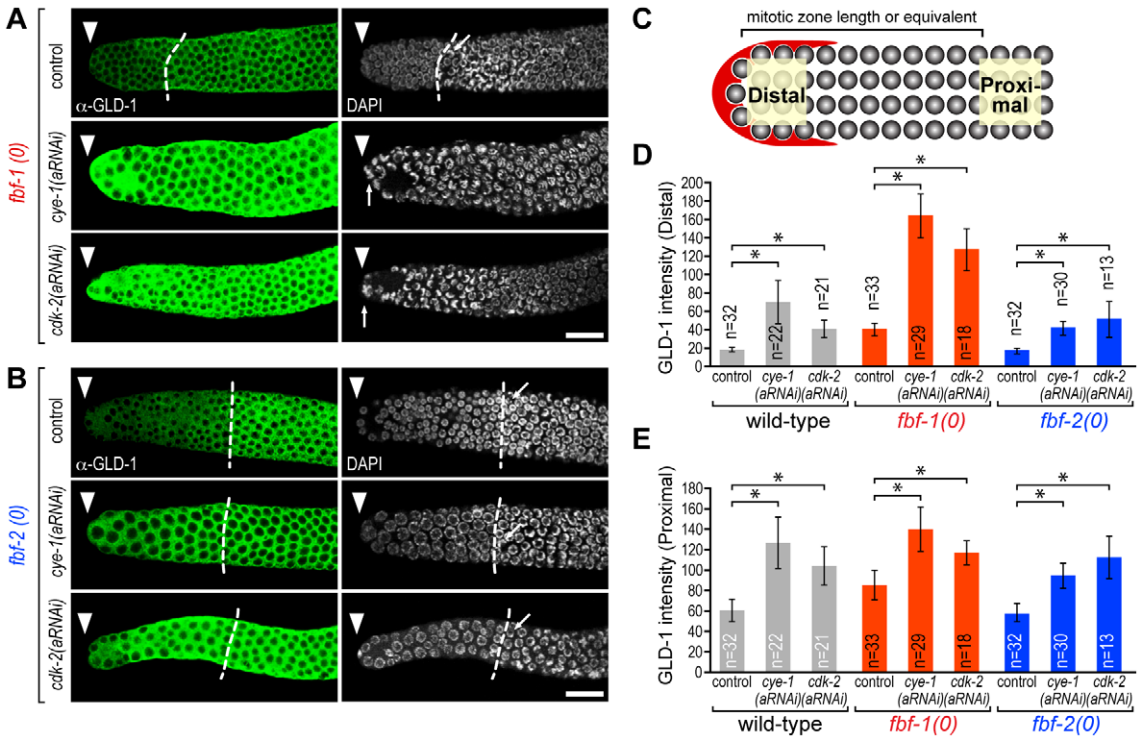

Figure 6. CYE-1/CDK-2 and FBF-1 work together to lower GLD-1 and to prevent meiotic entry in the germline stem cell pool. (A,B) Dissected gonads stained after aRNAi; conventions same as in Figure 2; germlines were treated identically and images taken at the same settings. Scale bar, 20 μm. (A) CYE-1/CDK-2 depletion in *fbf-1* single mutants. Whereas control distal germlines appear wild-type (top), most *fbf-1; cye-1(aRNAi)* (middle) and *fbf-1; cdk-2(aRNAi)* (bottom) germlines have abundant GLD-1 to the distal end and also have lost nuclei typical of the mitotic cell cycle and gained crescent-shaped nuclei typical of meiotic prophase all the way to the distal end (73%, n = 70). (B) CYE-1/CDK-2 depletion in *fbf-2* single mutants. The effects of CYE-1/CDK-2 depletion in *fbf-2* single mutants are similar to those seen in wild-type (compare to Figure 2). (C–E) GLD-1 quantitation in confocal images measured using ImageJ, averaged, and plotted. Error bars indicate 95% confidential limits; asterisks denote a statistically significant difference with $p<0.002$ using Student's *t*-test. (C) Quantitation was done at two sites: the distal-most germ cells (Distal) and more proximal germ cells (Proximal). The proximal site was located just beyond the MZ/TZ boundary in those germlines with a boundary; however in *fbf-1; cye-1*(*aRNAi*) and *fbf-1; cdk-2*(*aRNAi*), no MZ/TZ boundary exists so this proximal site was defined arbitrarily as 12 germ cell diameters from the distal end. (D) GLD-1 abundance at the distal-most site, quantitated in strains as noted. (E) GLD-1 abundance at the more proximal site, quantitated in strains as noted.
doi:10.1371/journal.pgen.1001348.g006

1 homolog, Sam68 (*S*rc-*a*ssociated in *m*itosis), during mitosis [65], implying a conserved link between proteins in the GLD-1 family and regulators of the cell cycle.

We suggest that CYE-1/CDK-2 phosphorylation of GLD-1 affects GLD-1 stability. This mechanism is attractive both for its simplicity and the existence of precedents [66,67]. Consistent with that idea, abundance of the trGLD-1(AAA) protein increased substantially over trGLD-1(wt) protein. However, the trGLD-1(AAA) increase was not as great as the GLD-1 increase in *cye-1(aRNAi)* or *cdk-2(aRNAi)* distal germlines (compare Figure 3A and Figure 5B). Furthermore, the trGLD-1(AAA) was further increased after *cye-1* depletion. Therefore, CYE-1/CDK-2 is likely to act on GLD-1 abundance by both direct and indirect mechanisms.

Mutual repression between GLD-1 and CYE-1/CDK-2

This work together with a previous study [23] reveals a double-negative feedback loop between CYE-1/CDK-2 and GLD-1 (Figure 7, blue shading). Mutual repression is a classical network motif and has been suggested to serve as a 'toggle switch' for controlling decisions between two states [reviewed in 68]. Here the two relevant states are the mitotic and meiotic cell cycles. CYE-1/CDK-2 represses GLD-1 to promote mitotic divisions [this work], and GLD-1 represses *cye-1* mRNA to promote meiotic progression [23]. However, loss of CYE-1 or CDK-2 does not flip germ cells from the mitotic to meiotic cell cycle; instead it shifts the balance between the two cycles in favor of meiotic entry. Therefore, the mutual repression between GLD-1 and CYE-1/CDK-2 does not provide a toggle switch on its own. We suggest instead that this CYE-1/CDK-2 and GLD-1 double-negative feedback loop contributes to the bi-stable switch between the mitotic and meiotic cell cycles and helps to maintain the normal balance between them.

The *C. elegans* mitosis/meiosis decision is influenced not only by CYE-1/CDK-2 and GLD-1 but also by a distinct double-negative feedback loop between Notch signaling and GLD-1 (Figure 7, yellow shading). Notch signaling promotes mitotic divisions through GLD-1 repression, albeit indirectly via the FBFs [15,30], while GLD-1 directly represses translation of the *glp-1*/Notch receptor mRNA [69]. Therefore, two circuits of mutual repression converge on GLD-1, one involving core cell cycle regulators and the other involving differentiation regulators. We suggest that this two-fisted mutual repression renders the switch more robust and helps to ensure that the two cell cycle programs are incompatible.

Mutual repression between key regulators of the cell cycle and cell differentiation is emerging as a theme of developmental control. In addition to the example reported here, other examples exist. One example is in developing skeletal muscle of mammals.

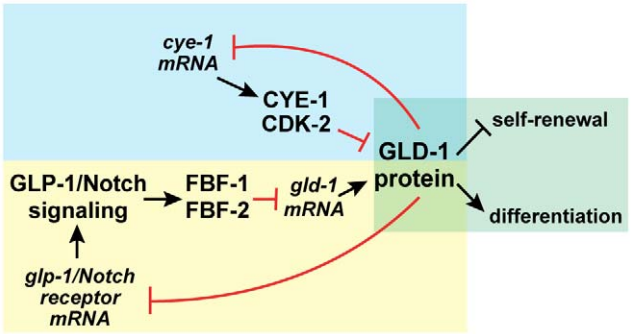

Figure 7. Two double negative feedback loops control GLD-1 abundance. Blue shading, mutual repression of GLD-1 and CYE-1/CDK-2; yellow shading, mutual repression of GLD-1 and the Notch/FBF arm of GLD-1 control; green shading, GLD-1 promotes meiotic entry and differentiation and it represses mitotic divisions and germline self-renewal.
doi:10.1371/journal.pgen.1001348.g007

MyoD activates expression of CDK inhibitors and thereby inhibits cell cycle progression; conversely, CDK1 or CDK2 phosphorylates MyoD and promotes its turnover to prevent cell differentiation [reviewed in 6]. A second example occurs in *Drosophila* neuroblasts. Prospero represses transcription of cell cycle regulators, including cyclin E, to block cell cycle progression [70,71], and conversely cyclin E inhibits Prospero by promoting its cortical localization [47]. Those two examples focus on mutual repression between cell cycle regulators and transcription factors. With this work, the mutual repression between GLD-1 and CYE-1/CDK-2 extends this important theme to translational regulators.

CYE-1/CDK-2 is a critical regulator of germline stem cell maintenance

A stem cell pool resides at the distal end of the adult germline [8,63]. The FBF-1 and FBF-2 proteins are well-established and largely redundant regulators of germline self-renewal: *fbf-1* and *fbf-2* single mutants maintain germline stem cells, but *fbf-1 fbf-2* double mutants do not – instead, their germline stem cells enter meiotic prophase and differentiate [15,30]. We have found that CYE-1/CDK-2 depletion in *fbf-1* single mutants similarly causes germline stem cells to enter meiotic prophase and differentiate. Therefore, CYE-1/CDK-2 emerges as a critical regulator of germline self-renewal.

The *cye-1/cdk-2* effect on germline self-renewal occurs in *fbf-1*, but not in *fbf-2* mutants. Why might this be true? One interpretation is that FBF-1 and CYE-1/CDK-2 function in parallel pathways, while FBF-2 and CYE-1/CDK-2 function together in the same pathway. We cannot exclude this idea, but suggest that an alternate explanation, which is based on FBF-specific effects of FBF cross-regulation, may be simpler. In *fbf-1* and *fbf-2* single mutants, the remaining FBF protein increases in abundance, but effects on distribution are different. The increased FBF-1 expands proximally in *fbf-2* mutants with the result that more germ cells than normal possess FBF; by contrast, the increased FBF-2 remains limited to a small region at the distal-most end in *fbf-1* mutants with the result that fewer germ cells than normal have FBF [30]. We suspect that this difference may result from a differential stability of FBF-1 and FBF-2 proteins, although this idea has not been tested. Regardless of the underlying mechanism, the spatially expanded FBF-1 may compensate for the loss of FBF-2 better than the spatially restricted FBF-2 can compensate for loss of FBF-1. This spatial difference could explain why GLD-1 expands distally in *fbf-1* but not *fbf-2* mutants [15] and why *cye-1(aRNAi)* has a synergistic effect with *fbf-1* but not *fbf-2* mutants (this work). Based on this reasoning, Figure 7 depicts FBF-1 and FBF-2 in one pathway and CYE-1/CDK-2 in a parallel pathway. However, we cannot exclude regulatory interactions between the FBF and CDK pathways.

Both FBF-1 and CYE-1/CDK-2 down-regulate GLD-1 in the germline stem cell pool (Figure 7) ([15,27] and this work). FBF-1 keeps GLD-1 low by its direct post-transcriptional repression of *gld-1* mRNA, while CYE-1/CDK-2 keeps GLD-1 low post-translationally. One simple idea is that GLD-1 must be increased to a critical threshold to switch from the mitotic cell cycle into meiotic prophase. Consistent with that idea, reduction of *gld-1* by one copy prevents entry into meiotic prophase in the distal germ cells of either an *fbf-1 fbf-2* double mutant or an *fbf-1; cye-1(aRNAi)* animal ([15] and this work). It is important to emphasize that other factors (e.g. GLD-2/GLD-3) also affect the decision [19,20]. Moreover, FBF-1 is a broad-spectrum regulator of >1000 mRNAs [17], with multiple targets that promote differentiation (e.g ERK/MAP kinase [16]). We suspect that CYE-1/CDK-2 may similarly have many substrates. Therefore the regulatory network depicted in Figure 7 is highly simplified: it highlights the two double-negative feedback loops that converge on GLD-1 but does not illustrate the complete network.

A central role for cyclin E and CDK2 in stem cell maintenance may be conserved. In human embryonic stem cells (hESCs), CDK2 promotes the G1/S transition and prevents differentiation, perhaps by maintaining a short G1 that is not subject to differentiation signals [49]. In addition, *Drosophila* CycE maintains neuronal stem cells by inhibiting the Prospero transcription factor, either directly or indirectly [47]. Our results support and extend this idea in several ways. Most importantly, our analysis places the *C. elegans* cyclin E and CDK2 homologs into the developmental pathway controlling self-renewal or differentiation. We identify a double-negative feedback loop between CYE-1/CDK-2 and GLD-1 that operates in parallel to a second double-negative feedback loop between Notch signaling and GLD-1. Although details will surely be different among the various stem cell systems, this regulatory logic provides a paradigm for the control of stem cell identity.

Materials and Methods

Nematode strains and RNA interference

All strains were derived from Bristol strain N2 and maintained at 20°C as described [72]. Mutants used in this work were: *cye-1(eh10)* [43], *gld-1(q485)* [58], *gld-1(q361)* [58], *gld-3(q730)* [73], *him-3(e1147)* [74], *nos-3(q650)* [75], *fbf-1(ok91)* [15], *fbf-2(q738)* [30], *eri-1(mg366)* [54], *rrf-1(pk1417)* and *rrf-3(pk1426)* [55]. Those mutants not viable as homozygotes were maintained in balanced strains: JK4057, *cye-1(eh10)/hT2[qIs48]*; JK3025, *gld-1(q485)/hT2[qIs48]*; JK4018, *gld-1(q361)/hT2[qIs48]*; JK3182, *gld-3(q730) nos-3(q650)/mIn1[mIs14 dpy-10(e128)]*.

RNA interference (RNAi) was performed essentially as described [76]. For adult RNAi, synchronized L4s were placed on NGM plates seeded with dsRNA-expressing or empty vector control bacteria, and incubated at 20°C.

Generation of transgenic lines

JK4117 (*cye-1/hT2[qIs48]*; *qIs134*): two DNAs (a PCR product harboring the wild-type *cye-1* genomic fragment with 1.2 kb 5′ and 854 bp 3′ flanking sequences and pTG96 carrying the $P_{sur\text{-}5}$::*GFP* co-transformation marker [77]) were co-injected into adult wild-type gonads to generate the *qEx660* extrachromosomal array.

qEx660 was integrated into a chromosome using UV-TMP [78] to generate *qIs134*, which was crossed to *cye-1(eh10)* to create JK4117.

trGLD-1(wt): pMM016 DNA (gift from T. Schedl) harbors (1) a wild-type genomic *gld-1* fragment that includes 1.1 kb 5′ and 1.5 kp 3′ flanking sequences and that was altered to include GFP- and FLAG-encoding sequences fused to the GLD-1 C-terminus and (2) *unc-119* to select for transformants. Microparticle bombardment was done using established protocols ([79] and T. Schedl lab protocol), with modifications. Briefly, 4 µg of linear plasmids were mixed with 40 µl of 0.1 M spermidine-treated 1 µm gold-beads (Bio-Rad) and 100 µl of 2.5 M $CaCl_2$; particles were transferred to the macrocarrier after ethanol washes and then bombarded as normal. The bombarded worms were collected with M9 buffer after 1 hr incubation at room temperature, placed on rich media plates, and grown at 20°C. Bombardment of pMM016 generated five independent transgenic lines, *qIs168 – qIs172*. All five had similar effects on GLD-1 abundance and distribution; JK4626 (*qIs170*) was selected for further analyses, including confirmation of *gld-1(q485)* rescue.

trGLD-1(AAA): pJK1571 DNA modifies three sites in pMM016 to encode GLD-1(S22A, S39A, and T348A)::GFP::FLAG. Bombardment generated five trGLD-1(AAA) lines, *qIs173 – qIs176* and *qIs182*. All five had similar effects on GLD-1 abundance and distribution; JK4630 (*qIs174*) was selected for further analyses, including confirmation of *gld-1(q485)* rescue.

Measuring mitotic zone size and mitotic index

Mitotic zone size was scored in DAPI-stained dissected gonads. We first identified the boundary between mitotic and transition zones, as described [11], and then counted germ cell diameters from the distal end to the boundary, or total number of germ cells within the mitotic zone. We measured mitotic index in extruded gonads stained with DAPI and antibodies to phosphohistone H3 (PH3), dividing the number of PH3-positive germ cells by the total number of DAPI-stained nuclei within the relevant region [11].

Immunostaining and quantification of GLD-1

Antibody staining was performed essentially as described [57], except we fixed tissues in 3% paraformaldehyde for 30 min. We used affinity purified antibodies against CYE-1 [43], REC-8 [80], HIM-3 [28], phosphohistone H3 (PH3; Cell Signaling), and GLD-1 [21], captured images on confocal (Carl Zeiss LSM 510) and compound (Carl Zeiss Axio Imager D1) microscopes, and processed them using ImageJ and Adobe Photoshop. To quantitate GLD-1, samples to be compared were processed in parallel, and confocal images were captured using the same settings. Raw images were opened and stacked in ImageJ and quantitated by measuring pixel intensity in a 5.12×5.12 µm square encompassing germ cells in the relevant location. Data were copied into Excel, averaged, and graphed.

In vivo GLD-1 phosphorylation

Synchronized wild-type or *gld-3 nos-3* animals were harvested at 24 hrs past the L4 stage and then washed 3× with M9 buffer and 1× with 50 mM Tris-Cl, 5 mM $MgCl_2$. Worm extracts were prepared with freeze-and-thaw cycles in liquid nitrogen; extracts were treated with Lambda Protein Phosphatase (λ PPtase, NEB), with or without phosphatase inhibitor cocktail (Thermo Scientific) at 37°C for 30 min. Phosphorylated and dephosphorylated GLD-1 were separated on 7.5% SDS-PAGE gels and visualized by Western blot using 1:1000 affinity-purified anti-GLD-1 (Rabbit) and 1:10,000 HRP-conjugated anti-rabbit antibodies.

Preparation of recombinant GLD-1

A full-length wild-type *gld-1* cDNA was cloned into pET-21b using *Sal* I and *Xho* I restriction sites to make pJK1341. To create pJK1347 (GLD-1 S22A, S39A, T348A), we changed the three consensus CDK phosphorylation sites in GLD-1 by site-directed mutagenesis (Stratagene). Primer sequences are available upon request. Recombinant proteins were expressed in BL21(DE3) (Novagen) cells by adding 0.1 mM IPTG and incubating 4 hrs at 30°C. Proteins were purified using Ni-NTA columns (Novagen) under native conditions using the manufacturer's protocol.

In vitro GLD-1 phosphorylation

The human cyclin E/CDK2 complex (Cell Signaling) was diluted in [20 mM MOPS (pH 7.5), 1 mM EDTA, 0.03% Brij-35, 5% glycerol, 1 mg/ml BSA, 0.1% beta-mercaptoethanol]. About 27 pmole of purified recombinant GLD-1 was incubated in [8 mM MOPS (pH 7.0), 1 mM EDTA with 0.92 pmole of cyclin E/CDK2 and 10 µCi of [gamma-32P]ATP] for 1 hr at room temperature, boiled in protein sample buffer, and separated on a 4–12% SDS-PAGE gel. Phosphorylation was visualized by autoradiography.

Supporting Information

Figure S1 CYE-1 effects on the mitotic zone, additional views. (A) After 72 or 96 hours of *cye-1* aRNAi treatment of wild-type hermaphrodites, germ cells degenerate in the region that had been the mitotic zone. Dissected gonads stained for HIM-3 (left) and DAPI (right). Open triangles indicate distal tip cells, which are somatic cells that do not express HIM-3. Other marks follow conventions of Figure 2: closed arrowheads mark the distal end, the dashed line marks the boundary between mitotic and transition zones and small arrows point to crescent-shaped germ cells. (B) The mitotic zone shortens after aRNAi in wild-type, L1 RNAi in *rrf-1(pk1417)* mutants and aRNAi in *eri-1(mg366)* and *rrf-3(pk1426)* mutants from L4 stage. Error bars indicate 95% confidence limits; one asterisk denotes a statistically significant difference ($p<9.0\times E^{-10}$ using Student's *t*-test).
Found at: doi:10.1371/journal.pgen.1001348.s001 (1.20 MB TIF)

Figure S2 CYE-1 promotes germline cell divisions autonomously. (A) Above, *cye-1* gene structure. Below: black shows extent of *cye-1* deletion in the *eh10* null allele [43]; red shows the region used to make the *q134* transgene. (B–D) Images include the somatically rescued strain JK4117 with genotype *cye-1(eh10); qIs134*. Specific genotypes labeled in the figure. (B) The *qIs134* transgene expresses CYE-1 in somatic but not germ cells. Embryos stained with anti-CYE-1 (red), anti-PGL-1 (green), and DAPI (blue); $P_{sur\text{-}5}$-GFP marks somatic nuclei; insets show germline precursor cells (PGCs). In wild-type (wt), PGCs co-express CYE-1 and PGL-1 (arrows); in *cye-1(0)* and *cye-1(0); qIs134*, PGCs express PGL-1 but not CYE-1 (arrowheads). (C) The *cye-1* transgene, *qIs134*, rescues somatic defect of *cye-1(0)* null mutants. Arrowheads indicate vulva in animals of each genotype at 24 hrs after L4. (D) CYE-1 autonomously regulates germ cell divisions. Top, DIC images of *cye-1* heterozygous (left) and homozygous (right) mutants with integrated transgenic *cye-1, qIs134*. Closed arrowhead indicates distal end of the gonad; open arrows point to embryos; small arrows mark enlarged nuclei. Middle and bottom, dissected gonads after staining with HIM-3 (middle) and DAPI (bottom).
Found at: doi:10.1371/journal.pgen.1001348.s002 (3.43 MB TIF)

Figure S3 *cye-1* aRNAi defects in the mitotic zone depend on functional GLD-1. *gld-1(q361)* is a point mutation that inactivates GLD-1 without affecting its stability [21,22,58]. (A) *gld-1(q361)*

homozygotes were treated with either control, *cye-1*, or *cdk-2* aRNAi for 48 hrs and then dissected and stained for GLD-1 (left) or DAPI (right). Confocal images of GLD-1 staining were stacked. Asterisks indicate sites of GLD-1 increase in the mitotic zone; arrowheads, distal end of gonad; scale bar, 20 μm. (B) Quantitation of GLD-1 abundance at the distal end of the gonad in *gld-1(q361)* homozygotes after control, *cye-1*, or *cdk-2* aRNAi. GLD-1 intensities were quantified and graphed. Error bars indicate 95% confidence limits; one asterisk denotes a statistically significant difference ($p<0.001$ using Student's *t*-test).
Found at: doi:10.1371/journal.pgen.1001348.s003 (0.86 MB TIF)

Figure S4 CYE-1 is depleted after *cye-1* aRNAi treatment of the *gld-1* null mutant. Dissected gonads stained for CYE-1 (left) or DAPI (right) in *gld-1(0)* mutants (above) or *gld-1(0)* mutants depleted for CYE-1 (below).
Found at: doi:10.1371/journal.pgen.1001348.s004 (0.99 MB TIF)

Figure S5 CYE-1 and GLD-1 distributions in wild-type and *gld-3(0) nos-3(0)* tumorous germline. (A, B) Dissected germlines were stained for CYE-1 (red), GLD-1 (green) and DAPI (blue). Arrowheads mark distal end and broken lines depict boundary between mitotic and transition zones. (A) Distal wild-type gonad. CYE-1 and GLD-1 distributions have little overlap in the mitotic zone. (B) *gld-3 nos-3* tumorous germline. The distribution of CYE-1 expands while that of GLD-1 shrinks.
Found at: doi:10.1371/journal.pgen.1001348.s005 (1.77 MB TIF)

Figure S6 GLD-1 removal in either one or two doses restores the mitotic zone to *fbf-1*; *cye-1(aRNAi)* germlines. Dissected germlines stained for CYE-1 (red) and DAPI (white). Arrowheads mark distal end and broken lines depict boundary between mitotic and transition zones. Top, CYE-1 is expressed normally in the *fbf-1(0); gld-1(0)* distal germline; middle and bottom, CYE-1 is depleted after *cye-1* aRNAi in *fbf-1(0)* mutants.
Found at: doi:10.1371/journal.pgen.1001348.s006 (0.74 MB TIF)

Figure S7 CDK-1 does not lower GLD-1 abundance in the distal gonad. (A) Dissected gonads with conventions and treatments as described in Figure 2 legend. Germlines were treated identically and GLD-1 images taken at the same settings. Scale bar, 20 μm. (B) Mitotic zone lengths. Error bars indicate 95% confidence limits. One asterisk denotes a statistically significant difference ($p<6.5\times E^{-5}$ using Student's *t*-test); two asterisks denote the lack of a statistically significant difference ($p>0.6$ using Student's *t*-test).
Found at: doi:10.1371/journal.pgen.1001348.s007 (0.76 MB TIF)

Figure S8 CDK phosphorylation influences both GLD-1 abundance in the distal germline and the mitotic zone length. (A) Distal end of dissected gonads. Left panels, stacked confocal images of GFP fluorescence to show abundance of transgenic GLD-1; right panels, DAPI staining to show distal end and mitosis/meiosis boundary. Solid triangle marks distal end; small v and larger V mark steps of comparable GLD-1 abundance; dashed line indicates boundary between mitotic and transition zones. Germlines were treated identically and confocal fluorescent images taken at the same settings and then stacked through Z-axis. Scale bar, 20 μm. (B) Quantitation of GFP intensity in the distal-most germline. Pixel intensity was measured using ImageJ and plotted using Microsoft Excel. Error bars indicate 95% confidence limits; asterisk denotes a statistically significant difference ($p<1.0\times E^{-5}$ using Student's *t*-test). (C) Mitotic zone length is reduced in *gld-1(0); trGLD-1(AAA)* compared to *gld-1(0); trGLD-1(wt)*. Error bars indicate 95% confidence limits; asterisk denotes a statistically significant difference ($p<3.85\times E^{-11}$ using Student's *t*-test).
Found at: doi:10.1371/journal.pgen.1001348.s008 (0.73 MB TIF)

Figure S9 CYE-1/CDK-2 represses GLD-1 abundance both directly and indirectly. (A–C) Conventions are same as Figure S8. (A) Dissected gonads treated aRNAi for 48 hrs from L4. TrGLD-1(AAA) in the mitotic zone increases and germ cell nuclei become enlarged after *cye-1* aRNAi. Left, stacked confocal images of GFP fluorescence; right panels, DAPI staining (right). (B) Quantitation of GFP intensity in the distal-most germline. Error bars indicate 95% confidence limits; asterisk denotes a statistically significant difference ($p<0.0003$ using Student's *t*-test). (C) Mitotic zone length, measured in gcd from the distal end, is reduced after *cye-1* aRNAi. Error bars indicate 95% confidence limits; asterisk denotes a statistically significant difference ($p<2.19\times E^{-8}$ using Student's *t*-test).
Found at: doi:10.1371/journal.pgen.1001348.s009 (0.86 MB TIF)

Acknowledgments

We are grateful to J. Pérez-Martín, O. Cinquin, and members of the JK laboratory for advice and discussion during this work. We thank T. Schedl for the plasmid to make GLD-1 transgenes; E. T. Kipreos, E. B. Goodwin, P. Pasierbek, and M. Zetka for antibodies; and the *Caenorhabditis* Genetics Center for strains. We also thank A. Helsley-Marchbanks and L. Vanderploeg for help preparing the manuscript and figures and P. Kroll-Conner and J. Forster for technical assistance.

Author Contributions

Conceived and designed the experiments: JJ JMV JK. Performed the experiments: JJ JMV. Analyzed the data: JJ JMV JK. Contributed reagents/materials/analysis tools: JJ. Wrote the paper: JJ JK.

References

1. Duronio RJ, O'Farrell PH (1995) Developmental control of the G_1 to S transition in *Drosophila*: cyclin Eis a limiting downstream target of E2F. Genes Dev 9: 1456–1468.
2. Lilly MA, Spradling AC (1996) The *Drosophila* endocycle is controlled by Cyclin E and lacks a checkpoint ensuring S-phase completion. Genes Dev 10: 2514–2526.
3. Tio M, Udolph G, Yang X, Chia W (2001) *cdc2* links the *Drosophila* cell cycle and asymmetric division machineries. Nature 409: 1063–1067.
4. Tilmann C, Kimble J (2005) Cyclin D regulation of a sexually dimorphic asymmetric cell division. Dev Cell 9: 489–499.
5. Lassar AB, Skapek SX, Novitch B (1994) Regulatory mechanisms that coordinate skeletal muscle differentiation and cell cycle withdrawal. Curr Opin Cell Biol 6: 788–794.
6. Kitzmann M, Fernandez A (2001) Crosstalk between cell cycle regulators and the myogenic factor MyoD in skeletal myoblasts. Cell Mol Life Sci 58: 571–579.
7. Budirahardja Y, Gönczy P (2009) Coupling the cell cycle to development. Development 136: 2861–2872.
8. Kimble J, Crittenden SL (2007) Controls of germline stem cells, entry into meiosis, and the sperm/oocyte decision in *Caenorhabditis elegans*. Annu Rev Cell Dev Biol 23: 405–433.
9. Dernburg AF, McDonald K, Moulder G, Barstead R, Dresser M, et al. (1998) Meiotic recombination in *C. elegans* initiates by a conserved mechanism and is dispensable for homologous chromosome synapsis. Cell 94: 387–398.
10. Hansen D, Hubbard EJA, Schedl T (2004) Multi-pathway control of the proliferation versus meiotic development decision in the *Caenorhabditis elegans* germline. Dev Biol 268: 342–357.
11. Crittenden SL, Leonhard KA, Byrd DT, Kimble J (2006) Cellular analyses of the mitotic region in the *Caenorhabditis elegans* adult germ line. Mol Biol Cell 17: 3051–3061.
12. Jaramillo-Lambert A, Ellefson M, Villeneuve AM, Engebrecht J (2007) Differential timing of S phases, X chomosome replication, and meiotic prophase in the *C. elegans* germ line. Dev Biol 308: 206–221.
13. Zhang B, Gallegos M, Puoti A, Durkin E, Fields S, et al. (1997) A conserved RNA-binding protein that regulates sexual fates in the *C. elegans* hermaphrodite germ line. Nature 390: 477–484.

14. Wickens M, Bernstein DS, Kimble J, Parker R (2002) A PUF family portrait: 3′UTR regulation as a way of life. Trends Genet 18: 150–157.
15. Crittenden SL, Bernstein DS, Bachorik JL, Thompson BE, Gallegos M, et al. (2002) A conserved RNA-binding protein controls germline stem cells in *Caenorhabditis elegans*. Nature 417: 660–663.
16. Lee M-H, Hook B, Pan G, Kershner AM, Merritt C, et al. (2007) Conserved regulation of MAP kinase expression by PUF RNA-binding proteins. PLoS Genet 3: e233. doi:10.1371/journal.pgen.0030233.
17. Kershner AM, Kimble J (2010) Genome-wide analysis of mRNA targets for *Caenorhabditis elegans* FBF, a conserved stem cell regulator. Proc Natl Acad Sci USA 107: 3936–3941.
18. Austin J, Kimble J (1987) *glp-1* is required in the germ line for regulation of the decision between mitosis and meiosis in C. elegans. Cell 51: 589–599.
19. Kadyk LC, Kimble J (1998) Genetic regulation of entry into meiosis in *Caenorhabditis elegans*. Development 125: 1803–1813.
20. Eckmann CR, Crittenden SL, Suh N, Kimble J (2004) GLD-3 and control of the mitosis/meiosis decision in the germline of *Caenorhabditis elegans*. Genetics 168: 147–160.
21. Jan E, Motzny CK, Graves LE, Goodwin EB (1999) The STAR protein, GLD-1, is a translational regulator of sexual identity in *Caenorhabditis elegans*. EMBO J 18: 258–269.
22. Lee M-H, Schedl T (2001) Identification of in vivo mRNA targets of GLD-1, a maxi-KH motif containing protein required for *C. elegans* germ cell development. Genes Dev 15: 2408–2420.
23. Biedermann B, Wright J, Senften M, Kalchhauser I, Sarathy G, et al. (2009) Translational repression of cyclin E prevents precocious mitosis and embryonic gene activation during *C. elegans* meiosis. Dev Cell 17: 355–364.
24. Wang L, Eckmann CR, Kadyk LC, Wickens M, Kimble J (2002) A regulatory cytoplasmic poly(A) polymerase in *Caenorhabditis elegans*. Nature 419: 312–316.
25. Suh N, Jedamzik B, Eckmann CR, Wickens M, Kimble J (2006) The GLD-2 poly(A) polymerase activates *gld-1* mRNA in the *Caenorhabditis elegans* germ line. Proc Natl Acad Sci USA 103: 15108–15112.
26. Hansen D, Wilson-Berry L, Dang T, Schedl T (2004) Control of the proliferation versus meiotic development decision in the *C. elegans* germline through regulation of GLD-1 protein accumulation. Development 131: 93–104.
27. Merritt C, Rasoloson D, Ko D, Seydoux G (2008) 3′ UTRs are the primary regulators of gene expression in the *C. elegans* germline. Curr Biol 18: 1476–1482.
28. Zetka MC, Kawasaki I, Strome S, Müller F (1999) Synapsis and chiasma formation in *Caenorhabditis elegans* require HIM-3, a meiotic chromosome core component that functions in chromosome segregation. Genes Dev 13: 2258–2270.
29. Merritt C, Seydoux G (2010) Transgenic solutions for the germline. In: The *C. Elegans* Research Community, editor (2010) WormBook, Available: http://www.wormbook.org, 10.1895/wormbook.1.148.1. Accessed February 8, 2010.
30. Lamont LB, Crittenden SL, Bernstein D, Wickens M, Kimble J (2004) FBF-1 and FBF-2 regulate the size of the mitotic region in the *C. elegans* germline. Dev Cell 7: 697–707.
31. Hunt T (1991) Cell biology. Cell cycle gets more cyclins. Nature 350: 462–463.
32. Nasmyth K (1993) Control of the yeast cell cycle by the Cdc28 protein kinase. Curr Opin Cell Biol 5: 166–179.
33. Nigg EA (1995) Cyclin-dependent protein kinases: key regulators of the eukaryotic cell cycle. BioEssays 17: 471–480.
34. Sherr CJ (1993) Mammalian G_1 cyclins. Cell 73: 1059–1065.
35. Park M, Krause MW (1999) Regulation of postembryonic G_1 cell cycle progression in *Caenorhabditis elegans* by a cyclin D/CDK-like complex. Development 126: 4849–4860.
36. Kipreos ET (2005) *C. elegans* cell cycles: invariance and stem cell divisions. Nat Rev Mol Cell Biol 6: 766–776.
37. Koreth J, van den Heuvel S (2005) Cell-cycle control in *Caenorhabditis elegans*: how the worm moves from G1 to S. Oncogene 24: 2756–2764.
38. van den Heuvel S (2005) Cell-cycle regulation. In:, , The *C. Elegans* Research Community, editor (2005) WormBook, Available: http://www.wormbook.org, 10.1895/wormbook.1.28.1. Accessed September 21, 2005.
39. Levine EM (2004) Cell cycling through development. Development 131: 2241–2246.
40. Sherr CJ (1994) G_1 phase progression: cycling on cue. Cell 79: 551–555.
41. Seydoux G, Savage C, Greenwald I (1993) Isolation and characterization of mutations causing abnormal eversion of the vulva in *Caenorhabditis elegans*. Dev Biol 157: 423–436.
42. Fay DS, Han M (2000) Mutations in *cye-1*, a *Caenorhabditis elegans* cyclin E homolog, reveal coordination between cell-cycle control and vulval development. Development 127: 4049–4060.
43. Brodigan TM, Liu J, Park M, Kipreos ET, Krause M (2003) Cyclin E expression during development in *Caenorhabditis elegans*. Dev Biol 254: 102–115.
44. Boxem M, Srinivasan DG, van den Heuvel S (1999) The *Caenorhabditis elegans* gene *ncc-1* encodes a *cdc2*-related kinase required for M phase in meiotic and mitotic cell divisions, but not for S phase. Development 126: 2227–2239.
45. Fujita M, Takeshita H, Sawa H (2007) Cyclin E and CDK2 repress the terminal differentiation of quiescent cells after asymmetric division in *C. elegans*. PLoS ONE 2: e407. doi:10.1371/journal.pone.0000407.
46. Berger C, Pallavi SK, Prasad M, Shashidhara LS, Technau GM (2005) A critical role for Cyclin E in cell fate determination in the central nervous system of *Drosophila melanogaster*. Nat Cell Biol 7: 56–62.
47. Berger C, Kannan R, Myneni S, Renner S, Shashidhara LS, et al. (2010) Cell cycle independent role of Cyclin E during neural cell fate specification in *Drosophila* is mediated by its regulation of Prospero function. Dev Biol 337: 415–424.
48. Wang ZA, Kalderon D (2009) Cyclin E-dependent protein kinase activity regulates niche retention of *Drosophila* ovarian follicle stem cells. Proc Natl Acad Sci USA 106: 21701–21706.
49. Neganova I, Zhang X, Atkinson S, Lako M (2009) Expression and functional analysis of G1 to S regulatory components reveals an important role for CDK2 in cell cycle regulation in human embryonic stem cells. Oncogene 28: 20–30.
50. Fay DS (2005) The cell cycle and development: lessons from *C. elegans*. Semin Cell Dev Biol 16: 397–406.
51. Crittenden SL, Troemel ER, Evans TC, Kimble J (1994) GLP-1 is localized to the mitotic region of the *C. elegans* germ line. Development 120: 2901–2911.
52. Kimble JE, White JG (1981) On the control of germ cell development in *Caenorhabditis elegans*. Dev Biol 81: 208–219.
53. McCarter J, Bartlett B, Dang T, Schedl T (1997) Soma – germ cell interactions in *Caenorhabditis elegans*: multiple events of hermaphrodite germline development require the somatic sheath and spermathecal lineages. Dev Biol 181: 121–143.
54. Kennedy S, Wang D, Ruvkun G (2004) A conserved siRNA-degrading RNase negatively regulates RNA interference in *C. elegans*. Nature 427: 645–649.
55. Sijen T, Fleenor J, Simmer F, Thijssen KL, Parrish S, et al. (2001) On the role of RNA amplification in dsRNA-triggered gene silencing. Cell 107: 465–476.
56. Kelly WG, Xu S, Montgomery MK, Fire A (1997) Distinct requirements for somatic and germline expression of a generally expressed *Caernorhabditis elegans* gene. Genetics 146: 227–238.
57. Jones AR, Francis R, Schedl T (1996) GLD-1, a cytoplasmic protein essential for oocyte differentiation, shows stage- and sex-specific expression during *Caenorhabditis elegans* germline development. Dev Biol 180: 165–183.
58. Jones AR, Schedl T (1995) Mutations in *gld-1*, a female germ cell-specific tumor suppressor gene in *Caenorhabditis elegans*, affect a conserved domain also found in Src-associated protein Sam68. Genes Dev 9: 1491–1504.
59. Songyang Z, Blechner S, Hoagland N, Hoekstra MF, Piwnica-Worms H, et al. (1994) Use of an oriented peptide library to determine the optimal substrates of protein kinases. Curr Biol 4: 973–982.
60. Endicott JA, Noble ME, Tucker JA (1999) Cyclin-dependent kinases: inhibition and substrate recognition. Curr Opin Struct Biol 9: 738–744.
61. Russo AA, Jeffrey PD, Patten AK, Massague J, Pavletich NP (1996) Crystal structure of the p27Kip1 cyclin-dependent-kinase inhibitor bound to the cyclin A-Cdk2 complex. Nature 382: 325–331.
62. Adams PD, Sellers WR, Sharma SK, Wu AD, Nalin CM, et al. (1996) Identification of a cyclin-cdk2 recognition motif present in substrates and p21-like cyclin-dependent kinase inhibitors. Mol Cell Biol 16: 6623–6633.
63. Cinquin O, Crittenden SL, Morgan DE, Kimble J (2010) Progression from a stem cell-like state to early differentiation in the *C. elegans* germ line. Proc Natl Acad Sci USA 107: 2048–2053.
64. Zielinska DF, Gnad F, Jedrusik-Bode M, Wisniewski JR, Mann M (2009) *Caenorhabditis elegans* has a phosphoproteome atypical for metazoans that is enriched in developmental and sex determination proteins. J Proteome Res 8: 4039–4049.
65. Resnick RJ, Taylor SJ, Lin Q, Shalloway D (1997) Phosphorylation of the Src substrate Sam68 by Cdc2 during mitosis. Oncogene 15: 1247–1253.
66. Montagnoli A, Fiore F, Eytan E, Carrano AC, Draetta GF, et al. (1999) Ubiquitination of p27 is regulated by Cdk-dependent phosphorylation and trimeric complex formation. Genes Dev 13: 1181–1189.
67. Liu E, Li X, Yan F, Zhao Q, Wu X (2004) Cyclin-dependent kinases phosphorylate human Cdt1 and induce its degradation. J Biol Chem 279: 17283–17288.
68. Hasty J, McMillen D, Collins JJ (2002) Engineered gene circuits. Nature 420: 224–230.
69. Marin VA, Evans TC (2003) Translational repression of a *C. elegans* Notch mRNA by the STAR/KH domain protein GLD-1. Development 130: 2623–2632.
70. Li L, Vaessin H (2000) Pan-neural Prospero terminates cell proliferation during *Drosophila* neurogenesis. Genes Dev 14: 147–151.
71. Choksi SP, Southall TD, Bossing T, Edoff K, de Wit E, et al. (2006) Prospero acts as a binary switch between self-renewal and differentiation in *Drosophila* neural stem cells. Dev Cell 11: 775–789.
72. Brenner S (1974) The genetics of *Caenorhabditis elegans*. Genetics 77: 71–94.
73. Eckmann CR, Kraemer B, Wickens M, Kimble J (2002) GLD-3, a Bicaudal-C homolog that inhibits FBF to control germline sex determination in *C. elegans*. Dev Cell 3: 697–710.
74. Hodgkin J, Horvitz HR, Brenner S (1979) Nondisjunction mutants of the nematode *Caenorhabditis elegans*. Genetics 91: 67–94.
75. Kraemer B, Crittenden S, Gallegos M, Moulder G, Barstead R, et al. (1999) NANOS-3 and FBF proteins physically interact to control the sperm-oocyte switch in *Caenorhabditis elegans*. Curr Biol 9: 1009–1018.
76. Timmons L, Court DL, Fire A (2001) Ingestion of bacterially expressed dsRNAs can produce specific and potent genetic interference in *Caenorhabditis elegans*. Gene 263: 103–112.
77. Suh N, Crittenden SL, Goldstrohm AC, Hook B, Thompson B, et al. (2009) FBF and its dual control of *gld-1* expression in the *Caenorhabditis elegans* germline. Genetics 181: 1249–1260.

78. Gengyo-Ando K, Mitani S (2000) Characterization of mutations induced by ethyl methanesulfonate, UV, and trimethylpsoralen in the nematode *Caenorhabditis elegans*. Biochem Biophys Res Commun 269: 64–69.
79. Praitis V, Casey E, Collar D, Austin J (2001) Creation of low-copy integrated transgenic lines in *Caenorhabditis elegans*. Genetics 157: 1217–1226.
80. Pasierbek P, Jantsch M, Melcher M, Schleiffer A, Schweizer D, et al. (2001) A *Caenorhabditis elegans* cohesion protein with functions in meiotic chromosome pairing and disjunction. Genes Dev 15: 1349–1360.